Kinetic and Thermodynamic Effects in the Self-Assembly of [3]Catenanes in the Solution and Solid States**

David B. Amabilino, Peter R. Ashton, J. Fraser Stoddart,*
A. J. P. White, and David J. Williams*

Abstract: A change in the constitution of the tetracationic cyclophane components (comprised of two paraquat residues bridged by either *m*- or *p*-phenylene rings) in [2]catenanes, where the other macrocyclic components are polyethers (incorporating two π-electron-rich rings, such as 1,4-dioxybenzene or 1,5-dioxynaphthalene, located symmetrically within a crown-10 structure) not only affects the efficiencies but also the selectivities associated with the self-assembly processes that lead to the formation of interlocked molecular compounds. The self-assembly of two new [2]catenanes—composed of cyclo(paraquat-*p*-phenylene – paraquat-*m*-phenylene) and either 1,5-dinaphtho-38-crown-10 (1/5DN38C10) or 1,5-naphtho-*p*-phenylene-36-crown-10 (1/5NPP36C10)—is accompanied by the formation, in each case, of a [3]catenane incorporating a dimer of the tetracationic cyclophane and one or other of the two macrocyclic polyethers. A mechanistic rationale, based on thermodynamic and kinetic considerations, is presented to explain the formation of the dimeric octacationic products. The X-ray crystal structures of the two [3]catenanes reveal the dominance of π – π stacking interactions both within the molecules and beyond them where highly distinctive brick-like and parquet-like packing motifs are observed.

Keywords: catenanes · crystal engineering · kinetic control · pi interactions · self-assembly

Introduction

The assistance of the noncovalent bond in controlling molecular synthesis[1] becomes highly significant when mechanically interlocked molecular compounds,[2] such as catenanes,[3] become the focus of attention of synthetic chemists. The mutual molecular recognition that exists[4] between π-electron-rich entities (e.g. dioxybenzene rings[5] and dioxynaphthalene ring systems[6]) and π-electron-deficient ones (e.g. bipyridinium units[7] and bipyridinium ethylene moieties[8]) has formed the basis of a very efficient approach to self-assembling catenanes[9] under conditions of kinetic control.[10, 11] The interactions which assist the formation of these exotic molecules are often revealed upon elucidation of their self-organized solid-state structures.[12]

Over the years since we first described the kinetically controlled self-assembly of a [2]catenane,[13] composed of the macrocyclic polyether bis-*p*-phenylene-34-crown-10 (BPP34C10) interlocked with the tetracationic cyclophane cyclobis(paraquat-*p*-phenylene), in a remarkably high yield of 70%, we have carried out many chemical modifications[2] to the constitutions of this catenane and asked ourselves: what are the consequences for i) the efficiency of the self-assembly process as well as for ii) the kinetics and thermodynamics of the motions and relationships between the two rings?[1] One constitutional change we carried out that led to an interesting development was the replacement of one of the two *p*-phenylene spacers in the tetracationic cyclophane component of the [2]catenane with a *m*-phenylene spacer.[14] Not only did we obtain the expected [2]catenane $\mathbf{1}\cdot 4\,PF_6$, but we also isolated small quantities ($\approx 0.5\%$) of a dimeric compound,[15] namely, the [3]catenane $\mathbf{2}\cdot 8\,PF_6$. Clearly, when *m*-xylylene

---

[*] Prof. J. F. Stoddart,[+] Dr. D. B. Amabilino,[§] P. R. Ashton
School of Chemistry, University of Birmingham
Edgbaston, Birmingham B15 2TT (UK)
Prof. D. J. Williams, Dr. A. J. P. White
Chemical Crystallography Laboratory
Department of Chemistry, Imperial College
South Kensington, London SW7 2AY (UK)
Fax: (+44) 171-594-5804

[+] Current address
Department of Chemistry and Biochemistry
University of California, Los Angeles, 405 Hilgard Avenue
Los Angeles, CA 90095 (USA)
Fax: (+1) 310-206-1843
E-mail: stoddart@chem.ucla.edu

[§] Current Address:
Institut de Ciència de Materials de Barcelona (CSIC)
Campus de la U.A.B., E-08193 Bellaterra (Spain)

[**] Molecular Meccano, Part 32. For Part 31, see R. Ballardini, V. Balzani, R. E. Gillard, J. F. Stoddart, E. Tabellini, previous paper in this issue.

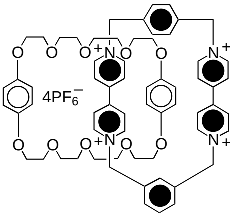

1.4PF$_6$

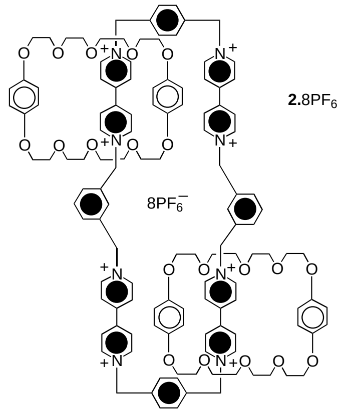

2.8PF$_6$

dibromide replaces the *para*-isomer in a reaction mixture where BPP3410 acts as a template in the reaction between 1,1′-[1,4-phenylenebis(methylene)]-bis(4,4′-pyridylpyridinium) bishexa-fluorophosphate (**3**$\cdot$2PF$_6$ in Scheme 1) and the dibromide, the propensity to form the catenated tetracationic cyclophane containing one *m*- and one *p*-phenylene spacer is considerably impaired. Indeed, we have established[10] that the templated formation of the tetracationic cyclophane present in **1**$^{4+}$ is a much slower process kinetically than the one which results in the formation[16] of cyclobis(paraquat-*p*-phenylene) in the "original" [2]catenane.[13]

Here, we present evidence that when the template-directed reactions are carried out between i) either **3**$\cdot$2PF$_6$ and the *m*-xylylene dibromide (**4**) or 1,1′-[1,3-phenylenebis(methylene)]-bis(4,4′-pyridylpyridinium) bishexafluorophosphate (**5**$\cdot$2PF$_6$ in Scheme 1) and the *p*-xylylene dibromide (**6**) both in the presence of 1,5-dinaphtho-38-crown-10 (1/5DN38C10)[17] and ii) between **5**$\cdot$2PF$_6$ and **6** in the presence of 1,5-naphtho-*p*-phenylene-36-crown-10 (1/5NPP36C10),[8, 18] in addition to the formation of the [2]catenanes **7**$\cdot$4PF$_6$ and **9**$\cdot$4PF$_6$, respectively, the dimeric [3]catenanes **8**$\cdot$8PF$_6$ and **10**$\cdot$8PF$_6$, respectively, are produced in low yields (Schemes 1 and 2). In the latter case, small quantities of the [4]catenane **11**$\cdot$8PF$_6$ were also isolated. We describe here the characterization by mass spectrometry, ^{1}H NMR spectroscopy, and X-ray crystallography of the new [3]catenanes incorporating the large octacationic cyclophane ring systems. We also discuss the significance of the formation of these products in terms of the kinetic control operating during these template-directed syntheses.

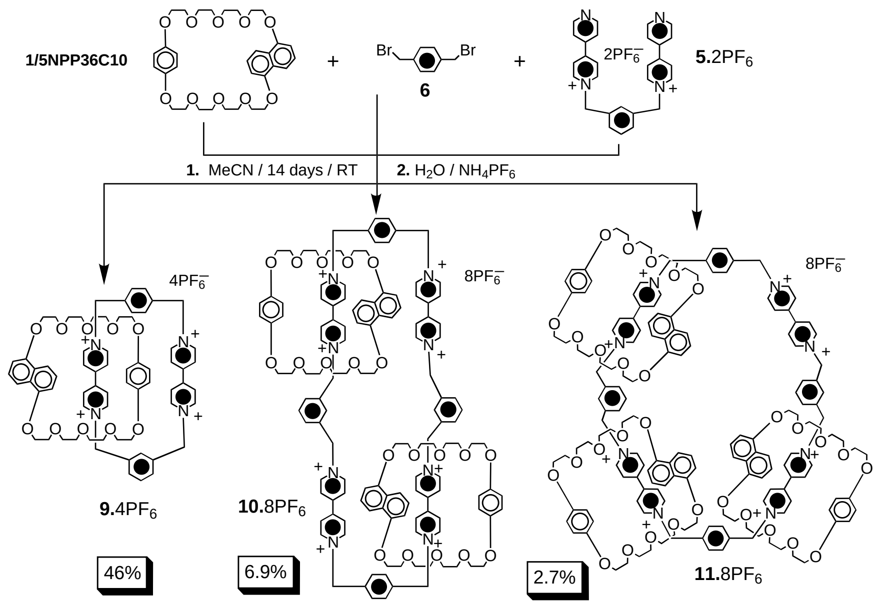

Scheme 2. The self-assembly of the [2]-, [3]-, and [4]catenanes **9**$\cdot$4PF$_6$, **10**$\cdot$8PF$_6$, and **11**$\cdot$8PF$_6$ in one pot.

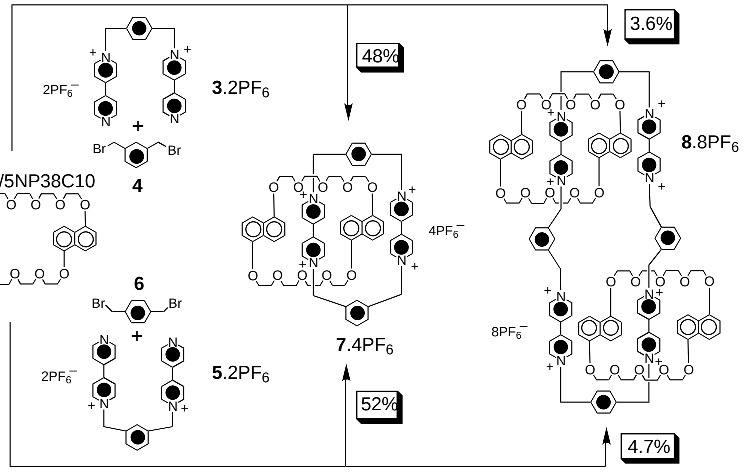

Scheme 1. The two routes to the one-step self-assembly of the [2]catenane **7**$\cdot$4PF$_6$ and its dimer, the [3]catenane **8**$\cdot$8PF$_6$.

Results and Discussion

Synthesis: The template-directed syntheses of the [2]-, [3]-, and [4]catenanes are summarized in Schemes 1 and 2. Reaction of **3**$\cdot$2PF$_6$ with **4** in MeCN in the presence of 1/5DN38C10 afforded, after column chromatography and counterion exchange, the [2]catenane **7**$\cdot$4PF$_6$ in 48% yield, together with its cyclic dimer, the [3]catenane **8**$\cdot$8PF$_6$, in 3.6% yield. When **5**$\cdot$2PF$_6$ (which incorporates a *m*-xylyl spacer between the pyridylpyridinium units) was treated with **6** under the same conditions, the yields of the [2]- and [3]catenanes rose very slightly to 52% and 4.7%, respectively. The higher yields associated with ring closures at the *p*-xylyl ends of the tetracationic and octacationic cyclophanes reflect a similar effect that operates even more dramatically when the poorer template BPP34C10 is used in the reaction.[14] When 1/5NPP36C10 was employed as the template for catenations with $\mathbf{5}\cdot2\,\mathrm{PF_6}$ and **6** under the same conditions, the yields of the [2]catenane $\mathbf{9}\cdot4\,\mathrm{PF_6}$ and the [3]catenane $\mathbf{10}\cdot8\,\mathrm{PF_6}$ were 46% and 6.9%, respectively. In addition, the [4]catenane $\mathbf{11}\cdot8\,\mathrm{PF_6}$, in which three macrocyclic polyethers are threaded around the octacationic cyclophane,[19] was isolated in 2.7% yield; thus, the total isolated yield of catenated products was approximately 56%.

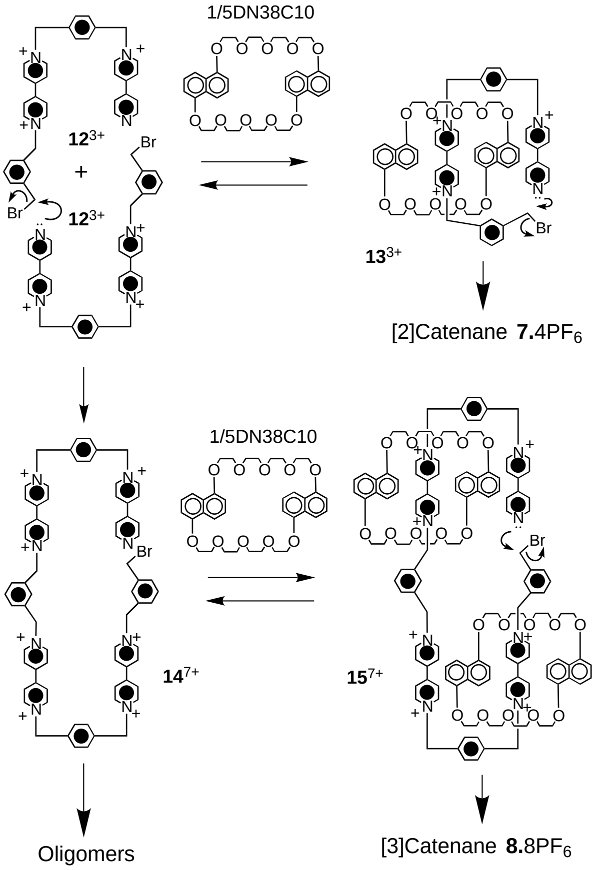

Scheme 3. The self-assembly processes leading to the [2]- and [3]catenanes $\mathbf{7}\cdot4\,\mathrm{PF_6}$ and $\mathbf{8}\cdot8\,\mathrm{PF_6}$.

The formation of the [3]catenanes in these template-directed reactions can be rationalized by considering the noncovalent and covalent bond forming steps in Scheme 3, which illustrates the situation that pertains when the template is 1/5DN38C10. The first step is a Menschutkin reaction between **4** and $\mathbf{3}\cdot2\,\mathrm{PF_6}$ which does not itself form a complex with the macrocyclic polyether under the reaction conditions.[16] It generates the tricationic intermediate $\mathbf{12}^{3+}$ which incorporates one 4,4′-bipyridinium unit that is capable of binding strongly with the macrocyclic polyether, thus forming the complex $\mathbf{13}^{3+}$. Its subsequent ring closure results in the creation of the [2]catenane $\mathbf{7}\cdot4\,\mathrm{PF_6}$. Alternatively, the intermediate $\mathbf{12}^{3+}$ may react intermolecularly with itself to form the higher homologue $\mathbf{14}^{7+}$. If the ring closure of $\mathbf{12}^{3+}$ to give the tetracationic cyclophane is a relatively fast process compared with the intermolecular covalent bond formation, a good yield of [2]catenane will be obtained. Indeed, when the corresponding π-electron-deficient component incorporates two *p*-phenylene spacers, an 83% yield of the [2]catenane $\mathbf{16}\cdot4\,\mathrm{PF_6}$ is obtained and *none* of the dimeric [3]catenane is formed. However, when the smaller tetracationic cyclophane with one *m*- and one *p*-phenylene spacer is targeted in the template-directed synthesis, the kinetics of the ring closure of $\mathbf{13}^{3+}$ are relatively slow.[10] Therefore, intermediates such as $\mathbf{14}^{7+}$, which contains three bipyridinium recognition sites and is, in principle, capable of binding at least three macrocyclic polyethers, will be generated. In the case where either 1/5DN38C10 or 1/5NPP36C10 is the reacting template, ring closure of intermediates of the type $\mathbf{15}^{7+}$ to form the [3]catenanes incorporating two macrocyclic polyethers and one octacationic cyclophane provides an alternative pathway to that which leads to the formation of the [2]catenanes. When 1/5NPP36C10 is the template, all the bipyridinium recognition sites of $\mathbf{14}^{7+}$ would have to be encircled by macrocyclic polyether molecules prior to cyclization in order to account for the formation of the resulting [4]catenane. However, the very low yield of this catenane suggests that this cyclization is not a highly competitive one. Indeed, the corresponding [4]catenane, incorporating 1/5 DN38C10, has not been isolated. The ring closure to form [3]catenanes of the type $\mathbf{8}\cdot8\,\mathrm{PF_6}$ is possibly stabilized as a result of some alongside interactions involving the bound macrocycles with the free bipyridinium units and is illustrated in the conveniently drawn form of the intermediate $\mathbf{15}^{7+}$ illustrated in Scheme 3. Indeed, the resulting [3]catenanes do exhibit such alongside interactions in the solid state (vide infra).

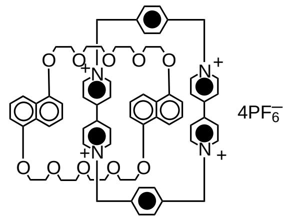

16.4PF$_6$

X-Ray crystallography: The X-ray analysis of $\mathbf{8}\cdot8\,\mathrm{PF_6}$ shows (Figure 1) that the octacationic cyclophane (some 70 atoms in circumference) has an extended geometry, the two *p*-xylyl rings being separated by about 23 Å. The cyclophane has C_i symmetry and has two 1/5DN38C10 macrocycles encircling two of the four bipyridinium units. The two parallel-aligned *m*-xylyl rings in the octacation are directed inwards toward

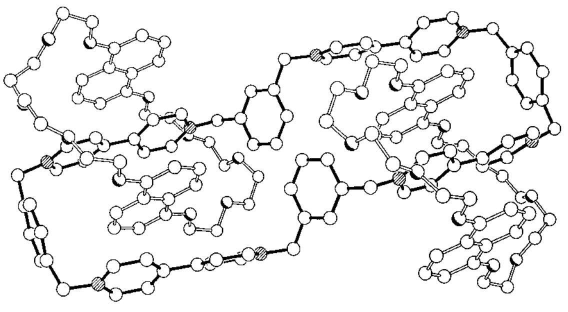

Figure 1. The [3]catenane molecule $\mathbf{8}\cdot8\,\mathrm{PF_6}$ in the solid state.

the symmetry center, the centroids of their rings being separated by 5.9 Å. The inside and alongside bipyridinium units have markedly different twist angles between their pyridinium rings, the value for the inside unit being 12° and that for the alongside unit 26°. The mean interplanar separations between the inside bipyridinium units and the alongside and inside 1,5-dioxynaphthalene ring systems are 3.50 and 3.49 Å, respectively, while the distance between the inside naphthalene ring and the alongside (twisted) bipyridinium unit is somewhat larger at 3.63 Å. In addition to the $\pi-\pi$ stacking interactions associated with these face-to-face separations (ca. 3.5 Å), there are edge-to-face $[C-H\cdots\pi]$ interactions between one of the peri hydrogen atoms of each inside 1,5-dioxynaphthalene ring system and their adjacent *p*-xylyl units ($[H\cdots\pi]$ 2.85 Å, $[C-H\cdots\pi]$ 147°). These $\pi-\pi$ interactions are supplemented by $[C-H\cdots O]$ hydrogen bonds involving i) α-bipyridinium hydrogen atoms and the central oxygen atoms of each outwardly facing polyether linkage ($[C\cdots O]$, $[H\cdots O]$ distances 3.16, 2.39 Å, $[C-H\cdots O]$ angle 137°) and ii) *m*-xylyl methylene hydrogen atoms and the central oxygen atoms of each inwardly facing polyether linkage ($[C\cdots O]$, $[H\cdots O]$ distances 3.27, 2.34 Å, $[C-H\cdots O]$ angle 163°).

The [3]catenane molecules pack to form a brick-like mosaic[20] (Figure 2) that is cemented in one direction by extended donor-acceptor $\pi-\pi$ interactions with the intermolecular stacking separation between the alongside 1,5-dioxynaphthalene ring system of one molecule and the alongside (twisted) bipyridinium unit of another being 3.35 Å (shorter than the intramolecular stacking distance of this unit). In the other direction, there is partial overlap between the C_i-related *p*-xylyl units of adjacent molecules with interplanar separations and ring centroid to ring centroid distances of 3.23 and 4.63 Å, respectively.

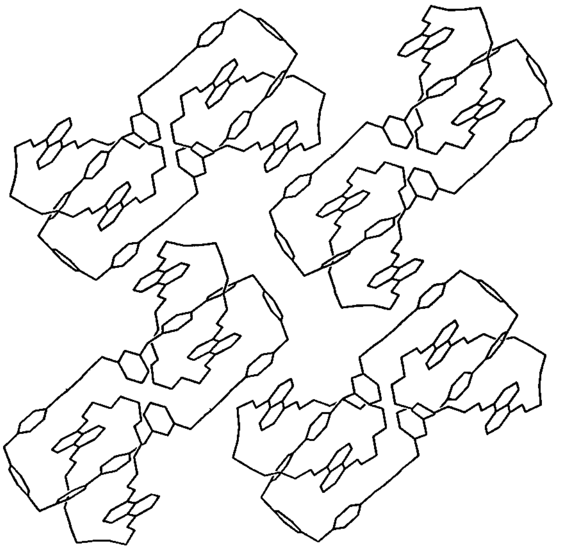

Figure 2. The brick-like packing pattern of the [3]catenane **8** · 8 PF_6 in the crystal.

The X-ray analysis of the [3]catenane **10** · 8 PF_6 (comprised of one octacationic cyclophane and two 1/5NPP36C10 macrocyclic polyethers incorporating both hydroquinone and 1,5-dioxynaphthalene π-donor units) shows a C_i-symmetric solid-state structure (Figure 3) that is dramatically different from that of **8** · 8 PF_6 where both π-donors in the neutral component are 1,5-dioxynaphthalenes. The macrocyclic polyethers once again encircle diametrically opposite bipyridinium units of the cyclophane, the 1,5-dioxynaphthalene ring systems being positioned outside and the hydroquinone rings inside. The interplanar separations between the inside bipyridinium units and the outside 1,5-dioxynaphthalene ring systems and the inside hydroquinone rings are 3.43 and 3.48 Å, respectively. The other bipyridinium units have a very large twist angle between their pyridinium rings of 48° (cf. 4° for the corresponding encircled units) and are folded significantly away from a parallel alignment with the inside hydroquinone rings. The pyridinium ring attached to the *m*-xylyl unit is inclined by 21° to the hydroquinone ring plane. There are no $[C-H\cdots\pi]$ interactions. However, there are pairs of $[C-H\cdots O]$ hydrogen bonds to the central oxygen atoms on each outwardly facing polyether linkage. One of these is from an α-bipyridinium hydrogen atom of the inside bipyridinium unit ($[C\cdots O]$, $[H\cdots O]$ distances 3.30, 2.45 Å, $[C-H\cdots O]$ angle 147°), while the other emanates from one of the methylene hydrogen atoms with distances and angles of 3.18, 2.24 Å, and 164°, respectively. The major difference between the structure of **10** · 8 PF_6 and that of **8** · 8 PF_6 is in the conformation of the octacationic cyclophane. In **8** · 8 PF_6, pairs of bipyridinium units linked through *p*-xylyl spacers are arranged in a U-shape around the π-electron-rich 1,5-dioxynaphthalene ring systems, whereas in **10** · 8 PF_6 it is the *m*-xylyl spacers that have taken on this role in the arrangment of the bipyridinium units in a U-shape around the π-electron-rich hydroquinone rings. Despite this major difference in geometry, the overall length of the octacationic cyclophane, as defined by the distance between the centers of the two *m*-xylyl units, is still about 23 Å.

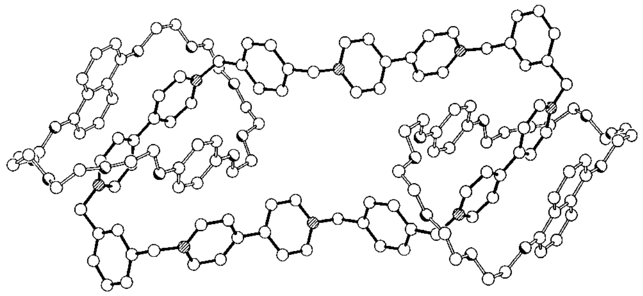

Figure 3. The [3]catenane molecule **10** · 8 PF_6 in the solid state.

The pattern of π-donor/π-acceptor stabilization within **10** · 8 PF_6 extends to include symmetry-related molecules in the crystal (Figure 4). The molecules pack to form an elegant parquet-like sheet mosaic, with the outside 1,5-dioxynaphthalene ring systems of one molecule positioned approximately parallel to and overlapping with one of the pyridinium rings of the bipyridinium unit of another, with a mean ring–ring interplanar separation of 3.48 Å.

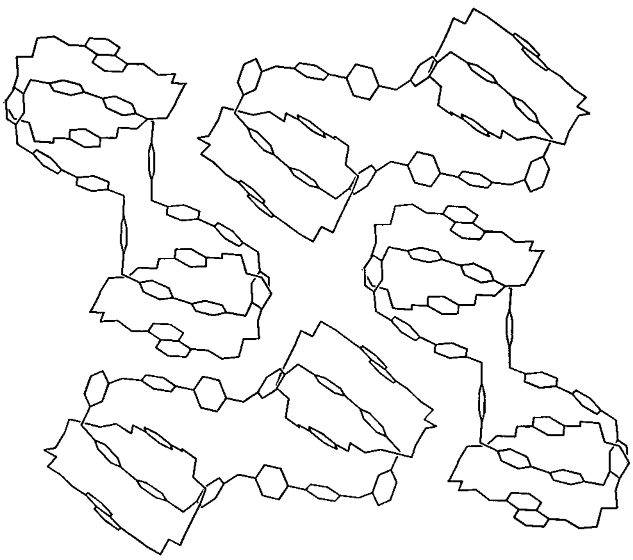

Figure 4. The parquet-like packing pattern of the [3]catenane $\mathbf{10}\cdot 8\,PF_6$ in the crystal.

Mass spectrometry of catenated structures: All the catenanes reported in this paper were characterized by fast atom bombardment (FAB) mass spectrometry. The spectra obtained were typical of this family of interlocked compounds.[19] The [2]catenanes gave signals corresponding to the singly positively charged ions, resulting from the loss of one, two, and three hexafluorophosphate ions, from the macrocyclic polyether components, and from fragments of the component tetracationic cyclophanes. The spectra obtained for the [3]- and [4]catenanes also gave signals for the successive loss of hexafluorophosphate ions, as well as fragments corresponding to the loss of one and then two macrocyclic polyether rings from the parent species. The [3]- and [4]catenanes $\mathbf{10}\cdot 8\,PF_6$ and $\mathbf{11}\cdot 8\,PF_6$ have peaks corresponding to the $[M^+ - PF_6]$ ions at *m/z* 3227 and 3814, respectively. As an example, the FAB mass spectrum of the $\mathbf{10}\cdot 8\,PF_6$ is illustrated in Figure 5.

^{1}H NMR spectroscopy of catenated structures: The five new catenanes all exhibit temperature dependencies in their NMR spectra as a result of dynamic processes taking place between the component positively charged cyclophanes and macrocyclic polyethers in their interlocked structures. At least two main dynamic processes take place in the [2]catenanes: Process I, the higher energy process, involves the equilibration of the inside and alongside π-electron rich units with respect to the cavity of the tetracationic cyclophane, while Process II, the lower energy process, involves the equilibration of the inside and alongside π-electron-deficient bipyridinium units.

The ^{1}H NMR spectrum of the [2]catenane $\mathbf{7}\cdot 4\,PF_6$ at $-30\,^{\circ}C$ in CD_3CN is extremely complex, and it is clear that both Processes I and II are slow on the ^{1}H NMR timescale at this temperature. The dissymmetric nature of the tetracationic cyclophane and the imposed local C_{2h} symmetry of the included 1,5-dioxynaphthalene unit result in single resonances for all the α-CH hydrogen atoms of the π-electron deficient bipyridinium units in the tetracationic component. In addition, all the hydrogen atoms attached to the inside 1,5-dioxynaphthalene ring system give separate resonances in the low-temperature spectrum of the compound. The values of the chemical shifts of these resonances are given in Figure 6, which shows a plausible geometry for the π-electron-rich unit located within the π-electron-deficient tetracationic cyclophane. It was not possible to calculate the free energies of activation for the dynamic processes taking place in this [2]catenane at higher temperatures, owing to the extreme complexity of the ^{1}H NMR spectrum. However, it is clear that at 50 °C Process II is rapid on the ^{1}H NMR timescale since only four resonances are observed for the α-CH bipyridinium protons in the tetracationic component; this fact also indicates that Process I is not occurring.

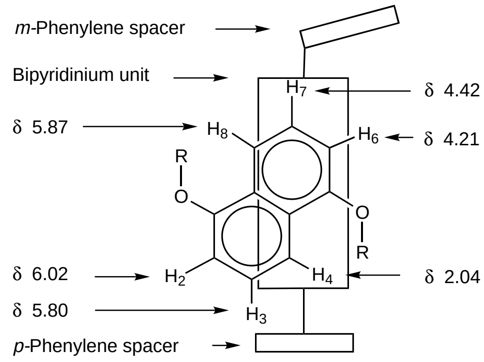

Figure 6. A schematic view of the orientation of the 1,5-dioxynaphthalene residue inside the cavity of the tetracationic cyclophane component of $\mathbf{7}\cdot 8\,PF_6$ and the associated chemical shifts of the resonances arising from its hydrogen atoms in the ^{1}H NMR spectrum at low temperature.

In contrast to the [2]catenane $\mathbf{7}\cdot 4\,PF_6$, the [3]catenane $\mathbf{8}\cdot 8\,PF_6$ has an extremely simple ^{1}H NMR spectrum at room temper-

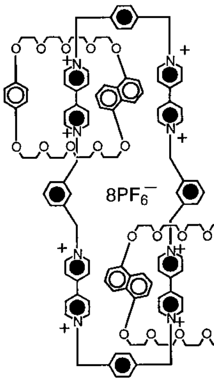

10.8PF6

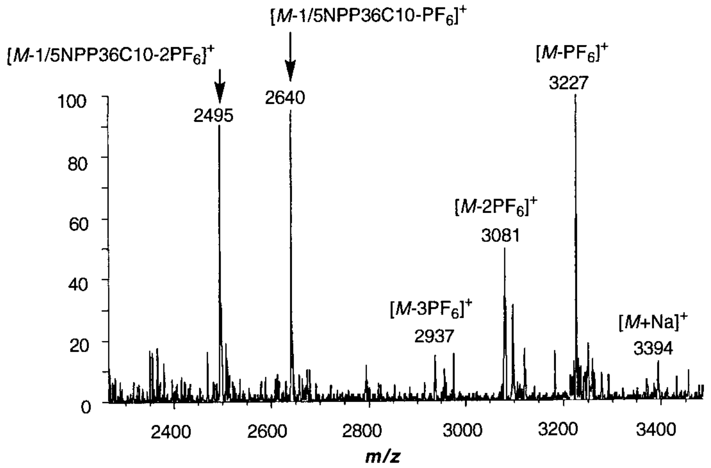

Figure 5. The FAB-MS spectrum of the [3]catenane $\mathbf{10}\cdot 8\,PF_6$.

0947-6539/98/0403-0464 $ 17.50+.50/0

ature, principally as a result of rapid equilibration of all the possible relative dispositions of the component rings on the ^{1}H NMR timescale. A comparison (Figure 7) of the ^{1}H NMR spectra **7**$\cdot$4PF$_6$ and **8**$\cdot$8PF$_6$ in CD$_3$CN at 50 °C emphasizes this point. When a CD$_3$CN/CD$_3$COCD$_3$ solution of the [3]catenane **8**$\cdot$8PF$_6$ was cooled down to −70 °C, broadening and separation of the peaks (without subsequent sharpening of them) was observed. The ease of relative movement of the components of this [3]catenane undoubtedly reflect the size and flexibility of the central octacationic cyclophane.

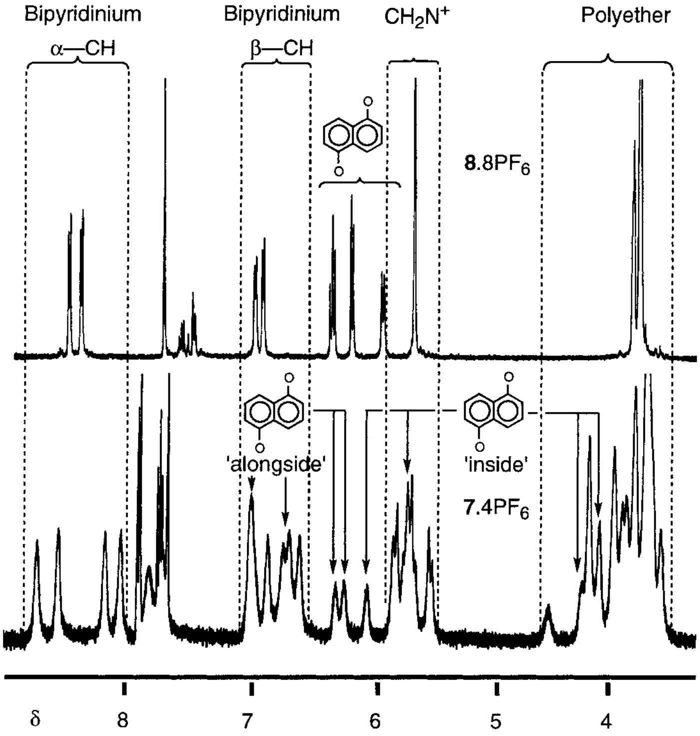

Figure 7. The partial ^{1}H NMR spectra of the [2]catenane **7**$\cdot$4PF$_6$ (bottom) and the [3]catenane **8**$\cdot$8PF$_6$ (top), both in CD$_3$CN at 50 °C.

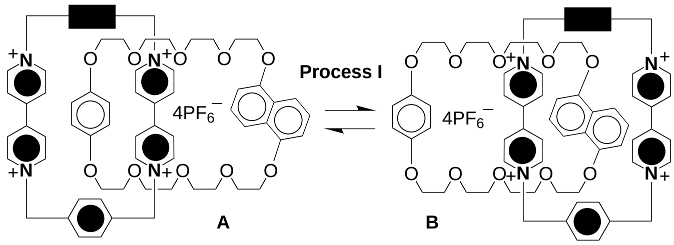

▬	A : B			
	CD_3COCD_3	CD_3COCD_3 : CD_3CN		CD_3CN
		60 : 40	40 : 60	
p-Phenylene	**70 : 30**	**60 : 40**	**55 : 45**	**–**
m-Phenylene (**9**.4PF$_6$)	**92 : 8**	**86 : 14**	**–**	**80 : 20**

Scheme 4. The two main dynamic processes taking place in the [2]catenanes in solution.

The ^{1}H NMR spectrum of the [2]catenane **9**$\cdot$4PF$_6$ at −40 °C in CD$_3$CN is also extremely complex, not only because of the dissymmetry present in the molecule, but also because two translational isomers[21,22] (Scheme 4) exist as one in which the hydroquinone ring occupies the cavity of the tetracationic cyclophane (**A**), and the other in which the 1,5-dioxynaphthalene ring system occupies this cavity (**B**). At −40 °C, both dynamic processes (I and II) are slow on the ^{1}H NMR timescale. However, warming up the sample to room temperature results in Process II becoming fast on the ^{1}H NMR timescale, giving a simpler spectrum from which it was possible to deduce the relative proportions of the two translational isomers. When compared with the closely related [2]catenane[18] in which both spacers in the tetracationic cyclophane are *p*-phenylene rings (Scheme 4), the cavity of the somewhat smaller cyclophane in **9**$\cdot$4PF$_6$ shows an even greater preference for occupancy by the hydroquinone ring of the macrocyclic polyether component.

The free energy of activation for Process II associated with the major isomer **A** of **9**$\cdot$4PF$_6$ was calculated[23] from the coalescence temperature ($T_c = -22.4\,^\circ$C) of the alongside naphthalene H$_{4,8}$ hydrogen atom resonances (limiting chemical shift difference $\Delta\tilde{\nu} = 50$ Hz) with an exchange rate constant, $k_c = 111\ s^{-1}$, in the Eyring equation. The $\Delta G_c^{\neq}$ value was found to be 12.2 kcal mol^{-1} in comparison with those of 12.2 and 12.7 kcal mol^{-1} for the [2]catenanes incorporating cyclobis(paraquat-*p*-phenylene) and BPP34C10[24] or 1/5 DN38C10,[25] respectively. The $\Delta G^{\neq}$ value for Process I (**B**$\rightarrow$**A**) of the [2]catenane **9**$\cdot$4PF$_6$ was estimated from the line broadening[25] of the alongside hydroquinone signal ($T = 44\,^\circ$C, $k = 22\ s^{-1}$) to be 16.6 kcal mol^{-1}, which compares with a value of 17.2 kcal mol^{-1} for the [2]catenane incorporating cyclobis(paraquat-*p*-phenylene) and 1/5DN38C10.

Both **10**$\cdot$8PF$_6$ and the **11**$\cdot$8PF$_6$ display time-averaged ^{1}H NMR spectra similar to that of **8**$\cdot$8PF$_6$. In contrast to the situation that exists in the solid-state structures of these [3]catenanes, the central octacationic cyclophane is not prone to adopt a well-ordered structure in solution at room temperature. It is interesting to note that the time-averaged resonance ($\delta = 5.68$) arising from the protons attached to the hydroquinone ring in **10**$\cdot$8PF$_6$ appears at lower field than that for **11**$\cdot$8PF$_6$ ($\delta = 5.57$), while the reverse situation is true for the resonances for the protons on the 2- and 6-positions of the 1,5-dioxynaphthalene ring systems ($\delta = 6.25$ and 6.47, respectively). This observation indicates that the smaller hydroquinone rings occupy the center of the octacationic cyclophane to a greater extent in the [4]- than in the [3]catenane, presumably as a result of steric interactions between inside 1,5-dioxynaphthalene ring systems. In addition, the chemical shift of the resonance ($\delta = 6.08$) arising from the protons attached to the alongside hydroquinone ring in the [2]catenane **9**$\cdot$4PF$_6$ (isomer **B**) occurs at much lower field than those for the time-averaged resonances of the analogous protons in either **10**$\cdot$8PF$_6$ or **11**$\cdot$8PF$_6$, indicating that the translational isomer of the [3]catenane **10**$\cdot$8PF$_6$, observed in the solid state, is significantly populated in solution. The chemical shift differences for the comparable resonances arising from the 1,5-dioxynaphthalene ring system protons in **9**$\cdot$4PF$_6$ and **10**$\cdot$8PF$_6$ are also consistent with this hypothesis.

Conclusions and Reflections

The dramatic effect that changing the constitutions of the components has upon the three fundamental properties of catenanes includes the following features:

- The self-assembly processes leading to the [2]catenanes **7**$\cdot 4PF_6$ and **9**$\cdot 4PF_6$, which can also be redirected toward the generation of higher order catenanes, such as **8**$\cdot 8PF_6$ and **10**$\cdot 8PF_6$.
- The positions of equilibria between translational isomers, for example, in the case of **9**$\cdot 4PF_6$.
- The packing, which is dominated by $\pi-\pi$ stacking interactions, in the solid state of the [3]catenanes **8**$\cdot 8PF_6$ and **10**$\cdot 8PF_6$.

These observations demonstrate how:

- Template-directed reactions can be steered in directions which are intuitively unlikely, with selectivities that are governed by *both* kinetic (covalent bond-forming) *and* thermodynamic (noncovalent bonding) factors—note that both the [3]catenane **10**$\cdot 8PF_6$ and the [4]catenane **11**$\cdot 8PF_6$ are formed with 1/5NPP36C10 as the template, while only the [3]catenane is formed with 1/5NP38C10. Meanwhile, the [2]catenane **16**$\cdot 4PF_6$ can be self-assembled under template control without any higher catenanes being formed.
- The positions of equilibria between translational isomers can be influenced dramatically by simply replacing a *p*-xylyl spacer in the tetracationic cyclophane by a *m*-xylyl unit—a feature which may be of considerable value in the design of molecular switches based on these catenated molecules.
- The intra- and intermolecular arrangements of the very large [3]catenane molecules in the solid state can be modified quite drastically by changing one of the units in the macrocyclic polyether components.

Experimental Section

Materials and methods: Solvents were purified where necessary according to literature methods. In particular, dimethylformamide (DMF) was distilled from CaH_2 under reduced pressure, and MeCN was distilled from P_2O_5 under N_2. 1,3-Bis(bromomethyl)benzene (**4**) and 1,4-bis(bromomethyl)benzene (**6**) were purchased from Aldrich and were used without further purification. The dications **3**$\cdot 2PF_6$[24] and **5**$\cdot 2PF_6$,[14] and the macrocyclic polyethers 1/5DN38C10[26] and 1/5NPP36C10[18] were prepared according to published procedures. Thin-layer chromatography (TLC) was performed on aluminum plates (10×5 cm) coated with Merck 5735 Kieselgel 60F. Developed plates were air-dried, scrutinized under a UV lamp, and stained in an iodine vapor tank where necessary. Kieselgel 60 (0.040–0.063 mm mesh, Merck 9385) was used to perform column chromatography. Melting points were determined on an Electrothermal 9200 melting point apparatus and are uncorrected. Mass spectra (MS) were obtained from either Kratos Profile or MS80RF instruments, the latter being equipped with a fast atom bombardment (FAB) facility (with a krypton primary atom beam in conjunction with a 3-nitrobenzyl alcohol matrix). FAB-MS spectra were recorded in the positive-ion mode at a scan speed of 30 s per decade. ^1H NMR spectra were recorded on Bruker AC300 (300 MHz) or AMX400 (400 MHz) spectrometers (with the deuterated solvent as lock and residual solvent or tetramethylsilane as internal reference). ^{13}C NMR spectra were recorded on a Bruker AC300 (75 MHz) or AMX400 (100 MHz) spectrometers with a JMOD pulse sequence (assuming $^1J_{CH} = 143$ Hz). Microanalyses were performed by the University of Birmingham Microanalytical Service. X-Ray crystallography was carried out as described in the appropriate compound characterization section. Crystallographic data (excluding structure factors) for the structures reported in this paper have been deposited with the Cambridge Crystallographic Data Centre as supplementary publication number CCDC-1220-53. Copies of the data can be obtained free of charge on application to CCDC, 12 Union Road, Cambridge, CB12 1EZ, UK (Fax: (+44) 1223-336-033; E-mail: deposit@ccdc.cam.ac.uk).

Self-assembly of the [2]catenane 7$\cdot$4PF$_6$ and [3]catenane 8$\cdot$8PF$_6$. *Method A*: The dication **3**$\cdot 2PF_6$ (82.1 mg, 0.12 mmol), 1,3-bis(bromomethyl)benzene (**4**, 32.9 mg, 0.13 mmol) and 1/5DN38C10 (125.5 mg, 0.20 mmol) were combined as solids, dry MeCN (8 mL) was added, and the resulting mixture was stirred for 14 days at ambient temperature and pressure. The solvent was then removed in vacuo, and the residue was dissolved in MeOH/2 M NH_4Cl (aq)/$MeNO_2$ (7:2:1) and subjected to silica gel column chromatography. The column was eluted with the same solvent mixture to afford the [2]catenane **7**$\cdot 4PF_6$, before the polarity of the eluant was increased with DMF/2M NH_4Cl(aq) (1:1) (2:1 ratio of the two solvent mixtures) in order to elute the [3]catenane **8**$\cdot 8PF_6$. Concentration in vacuo of the eluant containing each product, followed by solubilization in H_2O and precipitation by the addition of NH_4PF_6, gave the crude products as their hexafluorophosphate salts. The [2]catenane **7**$\cdot 4PF_6$ was purified by crystallization: vapor diffusion of iPr$_2$O into an MeCN solution of the product afforded dark purple needle-like crystals (96.6 mg, 48%, m.p. > 300 °C) which were unsuitable for X-ray diffraction studies. FAB-MS: $m/z = 1591$ $[M^+ - PF_6]$, 1446 $[M^+ - 2PF_6]$, 1302 $[M^+ - 3PF_6]$; ^1H NMR (CD_3CN, 400 MHz, −30 °C): $\delta = 2.04$ (d, $J = 8$ Hz, 1H, H4 of naphth. inside), 3.46–4.46 (m, 33H, CH_2O, H6,7 of naphth. inside), 4.53–4.63 (m, 1H, CH_2O), 5.55–5.60 (m, 2H, CH_2N^+), 5.64–6.03 (m, 8H, CH_2N^+, H3,8 of naphth. inside), 6.13 (d, $J = 8$ Hz, 1H, H2 of naphth. inside), 6.25–6.50 (m, 5H, H2,6 of naphth. alongside, β-CH), 6.71 (d, $J = 6$ Hz, 1H, β-CH), 7.00–7.24 (m, 6H, H3,7 and H4,8 of naphth. alongside, β-CH), 7.28 (d, $J = 6$ Hz, 1H, β-CH), 7.37 (d, $J = 6$ Hz, 1H, β-CH), 7.73–7.97 (m, 5H, xylyl), 8.02–8.16 (m, 4H, xylyl and α-CH), 8.23 (d, $J = 6$ Hz, 1H, α-CH), 8.42 (d, $J = 6$ Hz, 1H, α-CH), 8.57 (d, $J = 6$ Hz, 1H, α-CH), 8.63 (d, $J = 6$ Hz, 1H, α-CH), 8.73 (d, $J = 6$ Hz, 1H, α-CH), 8.84 (d, $J = 6$ Hz, 1H, α-CH), 9.09 (d, $J = 6$ Hz, 1H, α-CH); ^{13}C NMR (CD_3CN, 101 MHz, 20 °C): $\delta = 65.7$ (2 C′s), 66.2 (2 C′s), 68.7, 68.8, 69.0, 69.2, 70.5, 70.8, 70.9, 71.0, 71.3, 71.6, 71.7, 71.9, 72.0, 72.1, 72.3 (2 C′s), 104.6, 105.3, 106.4, 106.8, 109.6, 111.0, 114.9, 124.3, 124.9 (b), 125.1, 126.3 (b), 126.5 (b), 126.6, 126.8, 127.7, 129.6, 132.2, 132.6, 134.1, 134.5, 135.2, 137.6, 144.5, 145.2 (b), 145.3 (b), 146.0 (b), 151.4, 152.0, 154.5, 154.5; $C_{72}H_{76}N_4O_{10}P_4F_{24} \cdot 2H_2O$ (1773.30): calcd C 48.77, H 4.55, N 3.16; found C 48.58, H 4.42, N 3.13. The [3]catenane was purified by crystallization: vapor diffusion of EtOAc into an MeCN/Me_2CO solution of the product afforded dark purple crystals of **8**$\cdot 8PF_6$ (7.3 mg, 3.6%, m.p. > 300 °C) which were suitable for single-crystal X-ray analysis. FAB-MS: $m/z = 3328$ $[M^+ - PF_6]$, 3183 $[M^+ - 2PF_6]$, 3037 $[M^+ - 3PF_6]$, 2892 $[M^+ - 4PF_6]$, 2691 $[M^+ - PF_6 - 1/5\text{-DN38C10}]$, 2546 $[M^+ - 2PF_6 - 1/5\text{-DN38C10}]$, 1910 $[M^+ - PF_6 - 2\,1/5\text{-DN38C10}]$, 1765 $[M^+ - 2PF_6 - 2\,1/5\text{-DN38C10}]$; ^1H NMR (CD_3CN, 400 MHz, 50 °C): $\delta = 3.70$–4.00 (m, 64H, OCH_2), 5.81 (s, 16H, N^+CH_2), 5.98 (d, $J = 8$ Hz, 8H, H4,8 of naphth.), 6.36 (d, $J = 8$ Hz, 8H, H2,6 of naphth.), 6.53 (t, $J = 8$ Hz, 8H, H3,7 of naphth.), 7.11 (d, $J = 7$ Hz, 8H, β-CH), 7.17 (d, $J = 7$ Hz, 8H, β-CH), 7.68 (d, $J = 6$ Hz, 4H, H4,6 of *m*-xylyl), 7.79 (t, $J = 6$ Hz, 2H, H5 of *m*-xylyl), 7.94 (s, 10H, H2 of *m*-xylyl and *p*-xylyl), 8.62 (d, $J = 7$ Hz, 8H, α-CH), 8.74 (d, $J = 7$ Hz, 8H, α-CH); ^{13}C NMR (CD_3CN, 101 MHz, 20 °C): $\delta = 65.0$, 65.7, 69.0, 70.9, 71.9, 72.0, 106.3, 113.4, 126.0, 126.1, 126.4, 127.0, 131.9, 132.2, 132.5, 133.0, 134.8, 137.1, 145.4, 145.7, 153.9. Crystal data for **8**$\cdot 8PF_6$: $C_{144}H_{152}N_8O_{20} \cdot 8PF_6 \cdot 10MeCN$, $M = 3885.0$, monoclinic, space group $P2_1/n$ (no. 14), $a = 18.174(5)$, $b = 26.497(7)$, $c = 21.878(4)$ Å, $\beta = 90.01(2)°$, $V = 10536(4)$ Å^3, $Z = 2$ (the molecule has crystallographic C_i symmetry), $\rho_{calcd} = 1.225\ g\,cm^{-3}$, $\mu(Cu_{K\alpha}) = 1.500\ mm^{-1}$, $F(000) = 4008$. A red block of dimensions $0.70 \times 0.67 \times 0.50$ mm was used. 13248 independent reflections were measured on a Siemens P4/PC diffractometer with $Cu_{K\alpha}$ radiation (graphite monochomator) with ω-scans. The structure was solved by direct methods, and though the [3]catenane was found to be ordered, on account of a lack of observed data (caused by poor crystal quality) only the nitrogen and oxygen atoms were refined anisotropically. The aromatic rings were optimized and refined as rigid bodies. Two of the four unique PF_6^- anions were found to be disordered with two partial occupancy orientations being identified in each case. Throughout the PF_6^- anions only the major occupancy atoms were refined anisotropically. The five unique solvent molecules were found to be disordered over nine sites of varying occupancy and were refined isotropically. The C–H hydrogen atoms were placed in calculated positions, assigned isotropic thermal parameters, $U(\mathrm{H}) = 1.2U_{\mathrm{eq}}(\mathrm{C})$ [$U(\mathrm{H}) = 1.5\,U_{\mathrm{eq}}(\mathrm{C{-}Me})$], and allowed to ride on their parent atoms. Refinement was by full-matrix least-squares based on F^2 to give $R_1 = 0.199$, $wR_2 = 0.521$ for 5951 independent observed reflections [$|F_o| > 4\sigma(|F_o|)$, $2\theta \leq 110°$] and 704 parameters.

*Method B***:** The same procedure described under Method A was employed, but with the dication **5**·2PF$_6$ (77.9 mg, 0.11 mmol) and 1,4-bis(bromomethyl)benzene (**6**, 29.0 mg, 0.11 mmol) in the presence of 1/5DN38C10 (129.5 mg, 0.20 mmol) in dry MeCN (8 mL). The same purification procedure gave the [2]catenane **7**·4PF$_6$ (98.9 mg, 52%) and the [3]catenane **8**·8PF$_6$ (8.9 mg, 4.7%).

Self-assembly of the [2]catenane 9·4PF$_6$, [3]catenane 10·8PF$_6$, and [4]catenane 11·8PF$_6$: The dication **5**·2PF$_6$ (127.8 mg, 0.18 mmol) was treated with **6** (49.0 mg, 0.19 mmol) in the presence of 1/5NPP36C10 (207.0 mg, 0.35 mmol) in dry MeCN (7 mL) by means of the same procedure described above for **7**·4PF$_6$ and **8**·8PF$_6$ under Method A. After work-up, column chromatography, and counterion exchange, the following compounds were obtained in order of elution from the column. The [2]catenane **9**·4PF$_6$ was purified by crystallization: vapor diffusion of *i*Pr$_2$O into an MeCN solution of the product afforded dark purple-red needle-like crystals (141 mg, 46%, m.p. > 300 °C). FAB-MS: *m/z* = 1542 [$M^+ - \mathrm{PF_6}$], 1397 [$M^+ - 2\mathrm{PF_6}$], 1252 [$M^+ - 3\mathrm{PF_6}$]; ^{1}H NMR (CD$_3$CN, 400 MHz, 23 °C; Note that because of the fractional occupancy of the two different translational isomers, integrals have noninteger values. In CD$_3$CN at room temperature the major (maj. hydroquinone (HQ) inside tetracationic cyclophane):minor (min. 1,5-dioxynaphthalene (NP) inside tetracationic cyclophane) ratio is 81:19): δ = 2.27 (d, J = 8 Hz, 0.19 H, min. NP inside), 3.26 (br d, 1.62 H, maj. Hq inside), 3.43–3.57 (m, 4 H, CH$_2$O), 3.64–4.23 (m, 28 H, CH$_2$O), 4.35 (br d, 1.62 H, maj. HQ inside), 4.40 (d, J = 8 Hz, 0.19 H, min. NP inside), 5.66 (s, 3.24 H, maj. CH$_2$N$^+$), 5.73 (s, 3.24 H, maj. CH$_2$N$^+$), 5.77–5.80 (br m, 0.38 H, min. CH$_2$N$^+$), 5.83 (d, J = 8 Hz, 0.19 H, min. NP inside), 5.91 (t, J = 8 Hz, 0.19 H, min. NP inside), 5.95–5.97 (br m, 0.19 H, min. NP inside), 5.98–6.02 (br m, 0.38 H, min. CH$_2$N$^+$), 6.08 (s, 0.76 H, min. HQ alongside), 6.23 (d, J = 8 Hz, 0.19 H, min. NP inside), 6.41 (d, J = 8 Hz, 1.62 H, maj. NP alongside), 6.99 (br d, 0.38 H, min. β-CH), 7.12 (br d, 0.38 H, min. β-CH), 7.22 (t, J = 8 Hz, 1.62 H, maj. NP alongside), 7.30 (d, J = 8 Hz, 1.62 H, maj. NP alongside), 7.31–7.60 (m, 7.24 H, maj., min. β-CH), 7.63 (s, 0.81 H, maj. H2 of *m*-xylyl), 7.77 (s, 3.24 H, maj. *p*-xylyl), 7.82 (t, J = 9 Hz, 0.81 H, maj. H5 of *m*-xylyl), 7.87 (br s, 0.19 H, min. H2 of *m*-xylyl), 7.93 (br s, 0.38 H, min. *p*xylyl), 7.97 (d, J = 9 Hz, 2.00 H, maj. H-4,6 of *m*-xylyl and min. H5 of *m*-xylyl), 8.03 (br s, 0.38 H, min. *p*-xylyl), 8.06 (d, J = 9 Hz, 0.38 H, min. H4,6 of *m*-xylyl), 8.36 (br d, 0.38 H, min. α-CH), 8.57 (br d, 0.38 H, min. α-CH), 8.58–8.78 (m, 6.48 H, maj. α-CH), 8.82 (br d, 0.38 H, min. α-CH), 8.88 (br d, 0.38 H, min. α-CH); ^{13}C NMR (CD$_3$CN:CD$_3$COCD$_3$ 2:1, 101 MHz, 20 °C, peaks given for major isomer only): δ = 65.1, 65.6, 67.0, 68.5, 70.2, 70.4, 70.8, 70.9, 71.4, 71.5, 72.0, 106.4, 114.8, 125.6, 125.8, 126.6, 126.7, 131.8, 133.0, 134.7, 134.8, 137.5, 145.0, 151.0, 154.3; $\mathrm{C_{68}H_{74}N_4O_{10}P_4F_{24} \cdot H_2O}$ (1705.22): calcd C 47.90, H 4.49, N 3.29; found C 47.75, H 4.56, N 3.36. The [4]catenane **11**·8PF$_6$ was purified by crystallization: vapor diffusion of *i*Pr$_2$O into an MeCN solution of the product afforded dark purple-red crystals (9.8 mg, 2.7%, m.p. > 300 °C). FAB-MS: *m/z* = 3814 [$M^+ - \mathrm{PF_6}$], 3669 [$M^+ - 2\mathrm{PF_6}$], 3524 [$M^+ - 3\mathrm{PF_6}$]; ^{1}H NMR (CD$_3$CN, 400 MHz, 50 °C): δ = 3.35–3.40 (m, 12 H, OCH$_2$), 3.53–3.59 (m, 12 H, OCH$_2$), 3.61–3.65 (m, 12 H, OCH$_2$), 3.66–3.71 (m, 12 H, OCH$_2$), 3.73–3.78 (m, 12 H, OCH$_2$), 3.79–3.83 (m, 12 H, OCH$_2$), 3.84–3.90 (m, 12 H, OCH$_2$), 3.94–4.01 (m, 12 H, OCH$_2$), 5.57 (s, 12 H, HQ), 5.87 (s, 16 H, CH$_2$N$^+$), 6.47 (dd, 6 H, J = 2, 8 Hz, H4,8 of NP), 6.68–6.73 (m, 12 H, H3,7 and H2,6 of NP), 7.47 (d, J = 7 Hz, 8 H, β-CH), 7.51 (d, J = 7 Hz, 8 H, β-CH), 7.58–7.63 (m, 6 H, *m*-xylyl), 7.78 (s, 2 H, H2 of *m*-xylyl), 7.83 (s, 8 H, *p*-xylyl), 8.73 (d, J = 7 Hz, 8 H, α-CH), 8.81 (d, J = 7 Hz, 8 H, α-CH). The [3]catenane **10**·8PF$_6$ was purified by crystallization: vapor diffusion of *i*Pr$_2$O into an MeCN solution of the product afforded dark purple-red crystals (21.2 mg, 6.9%, m.p. > 300 °C) suitable for X-ray diffraction studies. FAB-MS: *m/z* = 3227 [$M^+ - \mathrm{PF_6}$], 3081 [$M^+ - 2\mathrm{PF_6}$]; ^{1}H NMR (CD$_3$CN, 400 MHz, 50 °C): δ = 3.40–3.45 (m, 8 H, OCH$_2$), 3.57–3.62 (m, 8 H, OCH$_2$), 3.67–3.73 (m, 8 H, OCH$_2$), 3.74–3.78 (m, 8 H, OCH$_2$), 3.79–3.83 (m, 8 H, OCH$_2$), 3.84–3.89 (m, 8 H, OCH$_2$), 3.90–3.94 (m, 8 H, OCH$_2$), 3.99–4.03 (m, 8 H, OCH$_2$), 5.68 (s, 8 H, HQ), 5.82 (s, 8 H, CH$_2$N$^+$), 5.83 (s, 8 H, CH$_2$N$^+$), 6.25 (d, J = 8 Hz, 4 H, H4,8 of NP), 6.42 (d, J = 8 Hz, 4 H, H2,6 of NP), 6.57 (t, J = 8 Hz, 4 H, H5,7 of NP), 7.54 (d, J = 7 Hz, 8 H, β-CH), 7.56 (d, J = 7 Hz, 8 H, β-CH), 7.64–7.70 (m, 6 H, *m*-xylyl), 7.80 (s, 2 H, H2 of *m*-xylyl), 7.82 (s, 8 H, *p*-xylyl), 8.77 (d, J = 7 Hz, 8 H, α-CH), 8.82 (d, J = 7 Hz, 8 H, α-CH). Crystal data for **10**·8PF$_6$: $\mathrm{C_{136}H_{148}N_8O_{20} \cdot 8PF_6 \cdot 4MeCN}$, M = 3538.6, monoclinic, space group *C*2/*c* (no. 15), a = 27.030(10), b = 27.181(9), c = 27.969(11) Å, β = 113.89(3)°, V = 18788(12) Å^3, Z = 4 (the molecule has crystallographic C_i symmetry), ρ_{calcd} = 1.251 g cm^{-3}, $\mu(\mathrm{Cu_{K\alpha}})$ = 1.621 mm^{-1}, $F(000)$ = 7280. A red rhomb of dimensions 0.60 × 0.40 × 0.37 mm was used. 11874 Independent reflections were measured on a Siemens P4/RA diffractometer with Cu$_{K\alpha}$ radiation (graphite monochromator) with ω-scans. The structure was solved by direct methods, and though the [3]catenane was found to be ordered, on account of a lack of observed data (caused by poor crystal quality) only the nitrogen and oxygen atoms were refined anisotropically. Similarly the aromatic rings were optimized and refined as rigid bodies. The four unique PF$_6$ anions were distributed over five sites, two of which having reduced occupancy because of crystallographic site symmetry requirements. Four of these five molecules were found to be disordered with, in each case, two partial occupancy orientations being identified. Throughout the PF$_6$ anions only the major occupancy atoms were refined anisotropically. The two unique solvent molecules were found to be disordered over four sites of varying occupancy and were refined isotropically. The C–H hydrogen atoms were placed in calculated positions, assigned isotropic thermal parameters, $U(\mathrm{H}) = 1.2U_{\mathrm{eq}}(\mathrm{C})$ [$U(\mathrm{H}) = 1.5\,U_{\mathrm{eq}}(\mathrm{C{-}Me})$], and allowed to ride on their parent atoms. Refinement was by full-matrix least-squares based on F^2 to give $R_1 = 0.198$, $wR_1 = 0.501$ for 5502 independent observed reflections [$|F_o| > 4\sigma(|F_o|)$, $2\theta \leq 111°$] and 728 parameters.

Self-assembly of the [2]catenane 16·4PF$_6$: The dication **3**·2PF$_6$ (59.2 mg, 848 µmol), **6** (24.2 mg, 92 µmol) and 1/5DN38C10 (110 mg, 173 µmol) were combined as solids. Dry MeCN (5 mL) was added, and the resulting mixture was stirred together for 14 days at ambient temperature and pressure. After work-up and purification as described above for **7**·4PF$_6$, Method A, the product (121 mg, 83%) was isolated as a purple solid which had identical analytical data to that described previously.[26]

Acknowledgements: This research was supported by the Engineering and Physical Sciences Research Council (EPSRC) in the UK.

Received: June 30, 1997 [F742]

---

[1] M. C. T. Fyfe, J. F. Stoddart, *Acc. Chem. Res.* **1997**, *30*, 393–401.

[2] D. B. Amabilino, J. F. Stoddart, *Chem. Rev.* **1995**, *95*, 2725–2828.

[3] M. Belohradsky, F. M. Raymo, J. F. Stoddart, *Collect. Czech. Chem. Commun.* **1997**, *62*, 527–557.

[4] For key papers describing π–π stacking interactions in general, see, along with references cited therein: a) T. Dahl, *Acc. Chem. Scand.* **1994**, *48*, 95–106; b) C. A. Hunter, *Chem. Soc. Rev.* **1994**, *23*, 101–109. For a review concerning charge-transfer interactions between neutral donors and charged acceptors specifically, see: c) V. E. Kamper, *Russ. Chem. Rev.* **1982**, *51*, 107–118.

[5] a) B. Odell, M. V. Reddington, A. M. Z. Slawin, N. Spencer, J. F. Stoddart, D. J. Williams, *Angew. Chem.* **1988**, *100*, 1605–1608; *Angew. Chem. Int. Ed. Engl.* **1988**, *27*, 1547–1550; b) P. L. Anelli, P. R. Ashton, N. Spencer, A. M. Z. Slawin, J. F. Stoddart, *ibid.* **1991**, *103*, 1052–1054 and **1991**, *30*, 1036–1039; c) P. R. Ashton, D. Philp, N. Spencer, J. F. Stoddart, *J. Chem. Soc. Chem. Commun.* **1991**, 1677–1679; d) P. R. Ashton, C. G. Claessens, W. Hayes, S. Menzer, J. F. Stoddart, A. J. P. White, D. J. Williams, *Angew. Chem.* **1995**, *107*, 1994–1997; *Angew. Chem. Int. Ed. Engl.* **1995**, *34*, 1862–1865.

[6] a) J.-Y. Ortholand, A. M. Z. Slawin, N. Spencer, J. F. Stoddart, D. J. Williams, *Angew. Chem.* **1989**, *101*, 1402–1404; *Angew. Chem. Int. Ed. Engl.* **1989**, *28*, 1394–1395; b) M. Asakawa, P. R. Ashton, W. Dehaen, G. L'abbé, S. Menzer, J. Nouwen, F. M. Raymo, J. F. Stoddart, M. S. Tolley, S. Toppet, A. J. P. White, D. J. Williams, *Chem. Eur. J.* **1997**, *3*, 772–787.

[7] a) A. P. H. J. Schenning, B. de Bruin, A. E. Rowan, H. Kooijman, A. L. Spek, R. J. M. Nolte, *Angew. Chem.* **1995**, *107*, 2288–2289; *Angew. Chem. Int. Ed. Engl.* **1995**, *34*, 2132–2134; b) M. T. Rojas, A. E. Kaifer, *J. Am. Chem. Soc.* **1995**, *117*, 5883–5884; c) P. R. Ashton, S. Menzer, F. M. Raymo, G. K. H. Shimizu, J. F. Stoddart, D. J. Williams, *Chem. Commun.* **1996**, 487–490; d) M. Asakawa, P. R.

Ashton, S. Menzer, F. M. Raymo, J. F. Stoddart, A. J. P. White, D. J. Williams, *Chem. Eur. J.* **1996**, *2*, 877–893.

[8] P. R. Ashton, R. Ballardini, V. Balzani, A. Credi, M. T. Gandolfi, S. Menzer, L. Pérez-García, L. Prodi, J. F. Stoddart, M. Venturi, A. J. P. White, D. J. Williams, *J. Am. Chem. Soc.* **1995**, *117*, 11171–11197.

[9] D. Philp, J. F. Stoddart, *Angew. Chem.* **1996**, *108*, 1242–1286; *Angew. Chem. Int. Ed. Engl.* **1996**, *35*, 1154–1196.

[10] D. B. Amabilino, P. R. Ashton, L. Pérez-García, J. F. Stoddart, *Angew. Chem.* **1995**, *107*, 2569–2572; *Angew. Chem. Int. Ed. Engl.* **1995**, *34*, 2378–2380.

[11] R. E. Gillard, F. M. Raymo, J. F. Stoddart, *Chem. Eur. J.* **1997**, *3*, 1933–1940.

[12] D. B. Amabilino, J. F. Stoddart, D. J. Williams, *Chem. Mater.* **1994**, *6*, 1159–1167.

[13] P. R. Ashton, T. T. Goodnow, A. E. Kaifer, M. V. Reddington, A. M. Z. Slawin, N. Spencer, J. F. Stoddart, C. Vicent, D. J. Williams, *Angew. Chem.* **1989**, *101*, 1404–1408; *Angew. Chem. Int. Ed. Engl.* **1989**, *28*, 1396–1399.

[14] D. B. Amabilino, P. R. Ashton, M. S. Tolley, J. F. Stoddart, D. J. Williams, *Angew. Chem.* **1993**, *105*, 1358–1362; *Angew. Chem. Int. Ed. Engl.* **1993**, *32*, 1297–1301.

[15] D. B. Amabilino, J. F. Stoddart, unpublished results.

[16] C. L. Brown, D. Philp, N. Spencer, J. F. Stoddart, *Isr. J. Chem.* **1992**, *32*, 61–67.

[17] P. R. Ashton, E. J. T. Chrystal, J. P. Mathias, K. P. Parry, A. M. Z. Slawin, N. Spencer, J. F. Stoddart, D. J. Williams, *Tetrahedron Lett.* **1987**, *28*, 6367–6370.

[18] P. R. Ashton, M. Blower, D. Philp, N. Spencer, J. F. Stoddart, M. S. Tolley, R. Ballardini, M. Ciano, V. Balzani, M. T. Gandolfi, L. Prodi, C. H. McLean, *New J. Chem.* **1993**, *17*, 689–695.

[19] A similar dimeric [4]catenane where the octacationic cyclophane component was a dimer of cyclobis(paraquat-4,4′-biphenylene) and the macrocyclic polyether was BPP34C10 has been isolated. See: D. B. Amabilino, P. R. Ashton, C. L. Brown, E. Córdova, L. Godínez, T. T. Goodnow, A. E. Kaifer, S. P. Newton, M. Pietraszkiewicz, D. Philp, F. M. Raymo, A. S. Reder, M. T. Rutland, A. M. Z. Slawin, N. Spencer, J. F. Stoddart, D. J. Williams, *J. Am. Chem. Soc.* **1995**, *117*, 1271–1293.

[20] Some related mosaic-like structures involving bipyridinium units and naphthalene residues have been reported; see: a) P. R. Ashton, D. Philp, N. Spencer, J. F. Stoddart, D. J. Williams, *J. Chem. Soc. Chem. Commun.* **1994**, 181–184; b) D. B. Amabilino, P. R. Ashton, J. F. Stoddart, S. Menzer, D. J. Williams, *ibid.* **1994**, 2475–2478.

[21] The concept of translational isomerism was introduced by: G. Schill, K. Rissler, H. Fritz, W. Vetter, *Angew. Chem.* **1981**, *93*, 197–201; *Angew. Chem. Int. Ed. Engl.* **1981**, *20*, 187–189.

[22] Translational isomerism has been observed in catenanes related to those described here. See refs. [18, 19] as well as: D. B. Amabilino, P. R. Ashton, G. R. Brown, W. Hayes, J. F. Stoddart, D. J. Williams, *J. Chem. Soc. Chem. Commun.* **1994**, 2479–2482.

[23] I. O. Sutherland, *Annu. Rep. NMR Spectrosc.* **1971**, *4*, 71–235.

[24] P.-L. Anelli, P. R. Ashton, R. Ballardini, V. Balzani, M. Delgado, M. T. Gandolfi, T. T. Goodnow, A. E. Kaifer, D. Philp, M. Pietraszkiewicz, L. Prodi, M. V. Reddington, A. M. Z. Slawin, N. Spencer, J. F. Stoddart, C. Vicent, D. J. Williams, *J. Am. Chem. Soc.* **1992**, *114*, 193–218.

[25] J. Sandström, *Dynamic NMR Spectroscopy*, Academic Press, London, **1982**.

[26] M. Asakawa, P. R. Ashton, S. E. Boyd, C. L. Brown, R. E. Gillard, O. Kocian, F. M. Raymo, J. F. Stoddart, M. S. Tolley, A. J. P. White, D. J. Williams, *J. Org. Chem.* **1997**, *62*, 26–37.